

Raman characterization of strain and composition in small-sized self-assembled Si/Ge dots

P. H. Tan,* K. Brunner,† D. Bougeard, and G. Abstreiter

Walter Schottky Institut, Technische Universität München, D-85748 Garching, Germany

(Received 5 February 2003; revised manuscript received 4 June 2003; published 4 September 2003)

A detailed Raman characterization of the structural properties of as-grown and annealed self-assembled Si/Ge dot multilayers is reported in this paper. Several new modes in as-grown or annealed Si/Ge dots and a frequency splitting of 4.2 cm^{-1} between the longitudinal (LO) and transversal optical (TO) Ge-Ge modes in as-grown Si/Ge dots are observed in Raman spectra. An average Ge content of 0.8 and lateral strain of -3.4% are consistently obtained from these spectral features for as-grown Si/Ge dots with a lateral size of about 20 nm and a height of about 2 nm. It suggests that a certain amount of intermixing between Si spacer layers and Si/Ge dots takes place for the Si/Ge dot multilayers. The annealing behavior of the Ge-Si mode in Si/Ge dots indicates that the observed sharp Ge-Si mode is a Ge-Si alloy mode within the core regions of Si/Ge dots, rather than a Ge-Si interface mode in the interface regions of dots. The phonon strain-shift coefficients of the Ge-Ge and Ge-Si modes are determined for the small-sized Si/Ge dots with a high Ge content under a biaxial strain condition. The results show that the LO-TO frequency splitting of the Ge-Ge mode and the frequencies of the Ge-Ge and Ge-Si modes can be used as an efficient way to determine the average strain and composition in uncorrelated small-sized Si/Ge dot multilayers in which the mean strain field is close to the biaxial case.

DOI: 10.1103/PhysRevB.68.125302

PACS number(s): 63.22.+m, 78.67.-n, 68.35.Fx, 68.65.-k

I. INTRODUCTION

To determine the strain and composition in strain-induced self-assembled Si/Ge dots is one of the most important issues in heteroepitaxial Si/Ge systems because the strain and composition distribution in Si/Ge dots is closely related to their optical and electronic properties.¹ In order to meet the demand of various classes of electronic and photonic devices, small-sized Si/Ge dots are produced by self-assembly during molecular beam epitaxy.¹⁻³ Self-assembled small-sized dots with a height of less than 3 nm usually have a high Ge composition because these dots are grown at a low substrate temperature.^{1,3} Recently, several models were used to calculate the strain distribution inside and around small-sized Si/Ge dots.⁴⁻⁶ The lateral strain ϵ_{xx} is found to be large inside Si/Ge dots. The frequencies of optical modes in nanostructures are determined by the confinement effect, strain, and composition in Si/Ge nanostructures. Therefore, the Raman scattering of optical modes is expected to be very useful to characterize Ge/Si nanostructures.^{1,2,7-10} However, there is little work to quantitatively analyze the strain and composition in small-sized Si/Ge dots due to the lack of values of the phonon strain-shift coefficients for the optical modes in high Ge-content Si/Ge nanostructures. In this work, in order to increase the Raman signals of Si/Ge dots and to avoid the vertical correlation of Si/Ge dots, 80 periods of Si/Ge dot layers separated by 25.0-nm Si layers are grown in a solid source molecular-beam epitaxy system.¹ Annealing is applied to the dot multilayer to obtain various Ge compositions in Si/Ge dots. It is found that the strain relaxation in Ge-rich regions of Si/Ge dot layers mainly results from the Si/Ge intermixing and that the variation of Si content and strain in the core regions of the as-grown and annealed dots is small. The optical phonon frequencies and the observed LO-TO splitting of the Ge-Ge mode in small-sized Si/Ge dots can be understood based on a biaxial strain model, and the phonon

strain-shift coefficients of the Ge-Ge and Ge-Si modes are obtained for Si/Ge dots with a high Ge content.

II. EXPERIMENT

The Si/Ge dot sample was grown in a solid source molecular-beam epitaxy system on (001)-oriented Si substrate. A Si buffer layer with a thickness of 150 nm was deposited on the substrate, followed by 80 periods of 8-ML (monolayers) Ge layers separated by 25-nm Si layers and a 100-nm Si cap layer. A second 80-period sample in which each 8-ML Ge was replaced by just 4-ML Ge was grown as a reference structure containing no islands but only wetting layers (WL). The growth of Si/Ge dots was carried out at a substrate temperature of 510 °C. An atomic force microscopy image of a reference structure shown in the inset of Fig. 1 reveals that the lateral size is about 20 nm, the height is about 2 nm, and the sheet density of Si/Ge dots is about $1.5 \times 10^{11} \text{ cm}^{-2}$. Si/Ge dots are not vertically correlated as the spacer layers are thicker than 14 nm.¹ Raman measurements are carried out in backscattering geometry with a spectral resolution of 3.8 cm^{-1} using a triple Raman spectrometer equipped with a liquid-nitrogen-cooled Si charge-coupled device camera. The 514.5-nm line of an argon ion laser focused to a spot size of about $1 \mu\text{m}$ has been used for excitation with a laser power of 1 mW. The labels x , y , z , x' , and y' used in the polarized Raman measurements refer to directions parallel to the $[1 0 0]$, $[0 1 0]$, $[0 0 1]$, $[1 -1 0]$, and $[1 1 0]$, respectively. The Raman spectrum of pure Si has been subtracted from the spectra of Si/Ge dots in the upper part of Fig. 1 and in Fig. 3.

III. RESULTS

Figure 1 shows the Raman spectra of the Si/Ge dot multilayer sample, the WL reference sample, (001) Si and

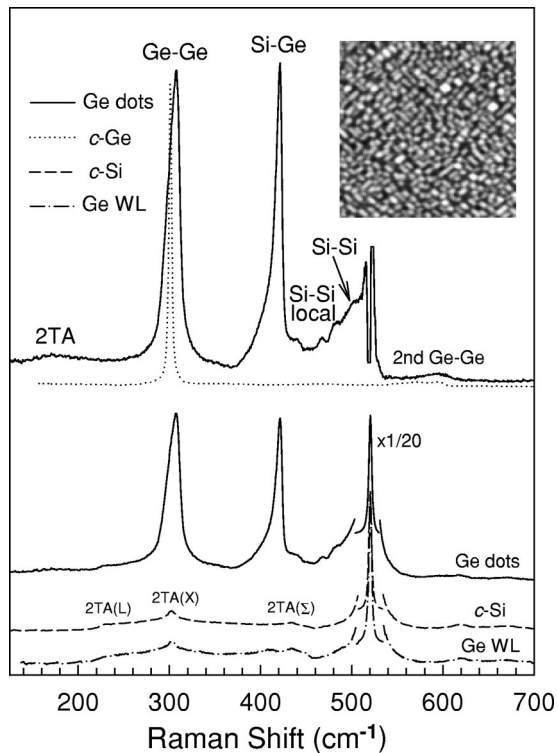


FIG. 1. Bottom: Raman spectra of a Si/Ge dot sample (solid lines), *c*-Si (dashed lines), and Ge WL reference sample (dash-dotted lines). Top: spectrum of Si/Ge dots with that of pure Si subtracted (solid line) and of *c*-Ge (dotted line). The inset shows the atomic force microscopy image ($400 \times 400 \text{ nm}^2$) of a reference Si/Ge dot sample.

(001) Ge substrates. In the bottom part of Fig. 1, the intensities of the Si longitudinal optical (LO) peak of a Si substrate and the WL reference sample are normalized to that of the Si/Ge dot sample. It is obvious that some spectral features in the Raman spectrum of Si/Ge dots and the WL reference samples are related to the Si layers,¹¹ such as the peaks at 225, 435, and 620 cm^{-1} , which originate from the two-phonon scattering of $2TA(L)$, $2TA(\Sigma)$, and a combination of optical and acoustic phonons in the Σ direction, respectively.¹² The frequency ($\sim 301 \text{ cm}^{-1}$) of the $2TA(X)$ overtone in Si substrate is also close to that of the first-order optical-mode in Ge bulk and Si/Ge dots. The much higher intensity and different frequency of the Raman line at about 307 cm^{-1} in Si/Ge dots, however, clearly indicate its Ge-Ge optical-mode nature. In contrary, for the 4-ML WL reference sample no clear Raman modes related to the wetting layers can be distinguished from the Raman spectrum of the Si substrate in the bottom part of Fig. 1. In order to get the intrinsic Raman spectra of Si/Ge dots and Ge WL, the spectrum of pure Si has been subtracted from the measured spectra. The remnant Raman spectrum for Si/Ge dots is shown in the upper part of Fig. 1 whereas no clear spectral features are obtained in the remnant Ge WL spectrum. For the Raman peaks of the dot sample above 200 cm^{-1} , three peaks are identified: Ge-Ge mode (307.5 cm^{-1}), Si-Ge mode (421.5 cm^{-1}), and second-order Ge-Ge mode (595 cm^{-1}). According to the experimental results of the 2TA mode in

SiGe alloys,^{13,14} the broad peak at $\sim 170 \text{ cm}^{-1}$ is assigned to Raman scattering from 2TA phonons in Si/Ge dots.

Regarding the high area density and the size of Ge dots, we estimate that about 60% of the surface is covered by dots (compare the inset of Fig. 1). For a Ge wetting layer width of 4 ML between dots, 80% of the Ge material is within the dots. As can be seen in Fig. 1, the Raman spectrum of WL reference sample is very similar to that of the Si substrate, except a small signal at 409 cm^{-1} from Si-Ge phonons in the Ge WL. Considering that the amount of Ge in WL reference sample is about 2.5 times as much as that in the WL regions of the dot sample, the Raman signal contributed from the WL in Si/Ge dot sample can be ignored. As a consequence, the Ge related Raman modes in Raman spectrum of the Si/Ge dot sample mainly originate from dots rather than from tiny wetting layer regions. This result can be further confirmed by our resonant Raman measurement and theoretical calculation, which show that the photon energy of 2.41 eV is close to the direct band gap E_0 of the studied Ge quantum dots and the Ge-Ge phonons in Si/Ge dots are resonantly enhanced by a 514.5-nm laser, whereas the Raman signal from Ge wetting layer is not enhanced in this case.¹⁵

The observed Ge-Ge mode in Si/Ge dot sample has a peak width of $\sim 15 \text{ cm}^{-1}$, which is typical for the Ge-Ge mode in Si/Ge superlattices and SiGe alloys.¹⁶ It indicates that the variation in strain between different dot layers and within the dots is small. For fully strained biaxial bulk Ge, the calculated frequency of Ge-Ge phonons can reach up to 319 cm^{-1} . The much lower frequency observed in the dot sample suggests that the strain in Si/Ge dots is partially relaxed and/or the Si/Ge dots contain a certain quantity of Si. The intensity and frequency of the second-order Ge-Ge mode depend on the Ge composition in SiGe alloys.¹⁴ The observation of a rather strong, well-defined second-order Ge-Ge mode at 595 cm^{-1} in the Raman spectra of the Si/Ge dot sample (see Fig. 1) indicates that the Si/Ge dots in the sample have a high Ge content. Previous works show that the frequency of the 2TA mode in unstrained SiGe alloys changes with the Ge content x_{Ge} from 160 cm^{-1} ($x_{\text{Ge}} = 1.0$) to 300 cm^{-1} ($x_{\text{Ge}} = 0$).^{13,14} Theoretical calculations show that the frequency of the TA phonons in *c*-Ge slightly decreases with compressive strain.¹⁷ Considering the strain-induced frequency decrease, the frequency of the observed 2TA mode is about 180 cm^{-1} in the unstrained case, which corresponds to a SiGe alloy with a Ge content x_{Ge} of 0.8.^{13,14} The Ge content x_{Ge} in Si/Ge dots ranges from about 0.5 to 1.0 for substrate temperatures of about 700 down to $500 \text{ }^\circ\text{C}$.¹⁸ The interdiffusion between Si/Ge dots and capping layer is dependent on the overgrowth temperature and a complete suppression of Ge/Si intermixing was found for a capping temperature of about $300 \text{ }^\circ\text{C}$.¹⁹ From the Raman measurement, we clearly show that a certain amount of interdiffusion between Si spacer layers and Si/Ge dots takes place during growth. The amount of 20% Si in Si/Ge dots mainly result from the significant Si-Ge intermixing at a growth temperature of $510 \text{ }^\circ\text{C}$.

After subtraction of the signal of pure Si, the remnant spectrum shows several weak features at 440, 468, 482, and 501 cm^{-1} . The peaks at 440, 468, and 482 cm^{-1} are attrib-

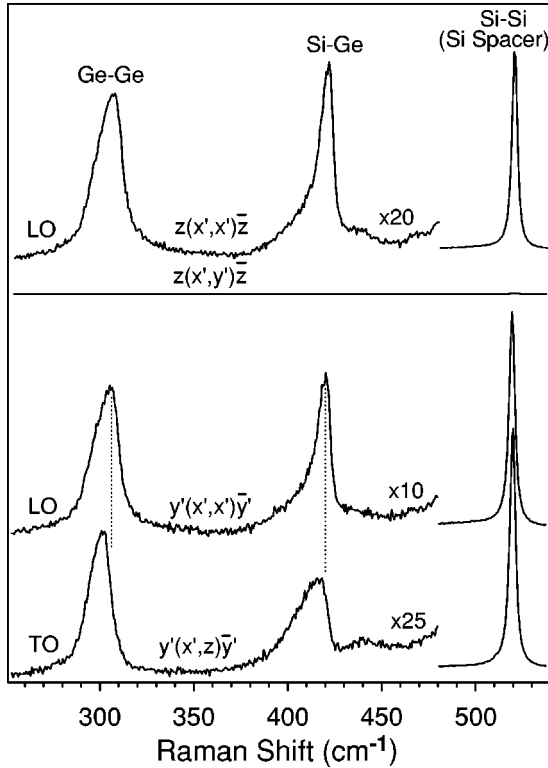


FIG. 2. Polarization dependence of Raman spectra of Si/Ge dot sample measured at the (001) plane (top) and the polished (110) plane (bottom). Two dashed lines are used to guide the eye to show the different frequencies of LO and TO modes.

uted to the localized Si-Si vibration in the neighborhood of one or more Ge atoms.²⁰ The localized Si-Si mode (Si-Si_{loc}) at 440 cm^{-1} can be clearly distinguished from the $2\text{TA}(\Sigma)$ mode of pure Si located at 435 cm^{-1} . A strong Si-Si_{loc} mode at $\sim 430 \text{ cm}^{-1}$ is typical for Si-rich SiGe alloys.²⁰ The weak intensity of the Si-Si_{loc} mode relative to that of the Ge-Ge mode suggests that there is a low Si content in Si/Ge dots. The frequencies of the observed three localized Si-Si peaks $440, 468,$ and 482 cm^{-1} are $15, 26,$ and 25 cm^{-1} higher than those in relaxed $\text{Si}_{0.2}\text{Ge}_{0.8}$ alloys,²⁰ respectively. The Si-Si alloy mode at 501 cm^{-1} in Fig. 1 is about 36 cm^{-1} higher than the frequency of the Si-Si mode in relaxed $\text{Si}_{0.2}\text{Ge}_{0.8}$ alloys. Its weak intensity suggests that this peak is not from the Si-rich regions around Si/Ge dots, but from the Ge-rich regions within Si/Ge dots. The considerable compressive strain in Si/Ge dots is believed to increase the frequencies of the localized Si-Si vibrations and optical Si-Si phonons in Si/Ge dots relative to relaxed SiGe alloys. The strain-induced frequency shift of an optical mode is proportional to the biaxial strain ϵ_{xx} in the (001) plane, $\Delta\omega = b\epsilon_{xx}$, where b is the phonon strain-shift coefficient of SiGe alloys. For the Si-Si mode, $b_{\text{Si-Si}} = -1050 \text{ cm}^{-1}$ when $x_{\text{Ge}} = 0.8$.²¹ Thus, an average strain of -3.4% is obtained for the Ge-rich regions in Si/Ge dots from the frequency shift of the Si-Si mode.

In order to further confirm the contributions of strain and composition on the optical modes in as-grown Si/Ge dots, we selectively probe the longitudinal and transverse polarizations using different geometries. Figure 2 shows the polar-

ized Raman spectra of the Si/Ge dot multilayers measured by backscattering from the (001) surface and the polished (110) plane. According to the selection rules for Raman scattering in bulk Si and Si/Ge superlattices,¹⁶ the LO phonons are Raman active in $z(x',x')\bar{z}$ configuration but all Raman modes are forbidden in $z(x',y')\bar{z}$ configuration. The LO and transversal optical (TO) phonons [with respect to (001) conventional backscattering] can be observed in $y'(x',x')\bar{y}'$ and $y'(x',z)\bar{y}'$ geometries, respectively. As seen from Fig. 2, the Raman selection rules in small-sized Si/Ge dots are similar to that in bulk Si and Si/Ge superlattices.¹⁶ There exists an obvious frequency splitting of 4.2 cm^{-1} between the LO and TO Ge-Ge phonon modes in Si/Ge dots measured at the (110) plane, which is a consequence of anisotropic strain in Si/Ge dots induced by Si substrate and spacer layers. To a first-order approximation, we only consider the biaxial strain like in a Si/Ge layer structure. The frequency splitting between LO and TO phonon modes induced by a biaxial strain in Si/Ge dots can be written as²²

$$\delta\omega_{split} = \frac{1}{2\omega_0} \frac{2C_{12} + C_{11}}{C_{11}} (q-p)\epsilon_{xx}, \quad (1)$$

where C_{12} and C_{11} are the stiffness coefficients, p and q are deformation potentials of the optical phonons in Ge, and ω_0 is the optical phonon frequency in bulk SiGe alloy. Using the parameters listed in Table I of Ref. 22, the average strain in Si/Ge dots obtained from the observed LO-TO frequency splitting is -3.5% . This value corresponds to a frequency shift by strain of 14.5 cm^{-1} for the LO phonon mode in Si/Ge dots. The frequency shift of the optical phonons in dots with respect to its bulk value (300.8 cm^{-1}) can be understood regarding three contributions: strain and composition in Si/Ge dots and the confinement effect of optical modes. For a Si/Ge dot with a thickness of 2 nm, the confinement-induced phonon frequency shift for the Ge-Ge mode is about -1 cm^{-1} .² We get that the frequency shift $\Delta\omega$ of the Ge-Ge mode due to Si presence in Si/Ge dots is about -6.2 cm^{-1} . Relative to the frequency of the Ge-Ge mode in c Ge, that in unstrained $\text{Si}_{1-x}\text{Ge}_x$ alloys decreases nearly linearly with x_{Ge} for large x_{Ge} : $\Delta\omega = -37(1 - x_{\text{Ge}}) \text{ cm}^{-1}$.²³ Then, a Ge content in Si/Ge dots of 0.82 is obtained from the above equation.

Figure 3 shows the Raman spectra of the as-grown Si/Ge dot sample and those annealed at 650, 700, and 800 °C for 1 h. As the annealing temperature increases, the frequency of the Ge-Ge mode shifts to lower frequency. This indicates that more Si diffuses into Si/Ge dots with increasing annealing temperature. In the low-frequency region, distinct sharp peaks up to 120 cm^{-1} and some weak features up to 180 cm^{-1} are observed. These peaks are assigned to the folded longitudinal acoustic (FLA) phonons in Si/Ge dot multilayer sample. The observation of such high-order FLA modes together with their sharp features reveals the formation of a high-quality superlattice with sharp interfaces. With the increase of the annealing temperature, the intensity of FLA phonons decreases and some high-order FLA modes disappear. This is clear evidence that there exists a significant

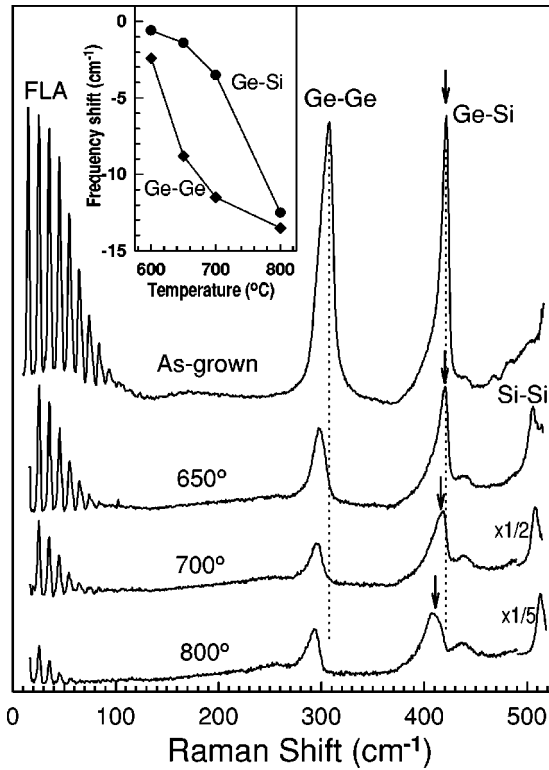


FIG. 3. Raman scattering of acoustic and optical phonons in as-grown Si/Ge dot sample and those annealed at 650, 700, and 800 °C for 1 h. Two vertical dotted lines are guides to the eye to show the frequency shift of Ge-Ge and Ge-Si phonons. Arrows show the calculated frequency of the Ge-Si alloy mode. The inset shows the frequency shift of Ge-Ge and Ge-Si phonons in annealed samples relative to the as-grown sample.

Si/Ge intermixing during the annealing process. Additionally, the Si-Si peak at $\sim 500 \text{ cm}^{-1}$ becomes stronger in Raman spectra of annealed samples. This peak shifts from 505 cm^{-1} to 514 cm^{-1} with an almost unchanged linewidth of 8.0 cm^{-1} when the annealing temperature increases from 650 to 800 °C. With the increase of annealing temperature, the Si content in the interface regions gradually changes from 1.0 of Si spacers to the value in the core regions of Si/Ge dots. A broadened Si-Si peak with an annealing-temperature-dependent linewidth is expected from these regions. The observation of a well-defined Si-Si mode with a constant linewidth at different annealing temperatures indicates that the mode at $\sim 500 \text{ cm}^{-1}$ is mainly from the core regions rather than interface regions of Si/Ge dots. The blue shift of the Si-Si peak is a result of the Si/Ge intermixing and strain relaxation at higher annealing temperature. The narrow width of the Si-Si peak suggests that the variation of Si content and strain in the core regions of Si/Ge dots is very small. Schorer *et al.*²⁴ observed a similar behavior in Raman spectra of annealed short-period Si/Ge layer superlattice structures and deduced a much larger diffusion constant of Si in Ge-rich regions than of Ge in Si-rich layers.

The Raman spectrum of the dot sample annealed at 800 °C shows typical spectral features of a Si-rich alloy.²⁰ The intensities of the Ge-Ge peak $I_{\text{Ge-Ge}}$ and the Si-Si mode

$I_{\text{Si-Si}}$ are found to be reliable to determine x_{Ge} using the below equation for a 514.5 nm excitation,²⁵

$$\frac{I_{\text{Ge-Ge}}}{I_{\text{Si-Si}}} = \frac{n_G + 1}{n_S + 1} \frac{\omega_{\text{Si-Si}}}{\omega_{\text{Ge-Ge}}} \frac{x_{\text{Ge}}^2}{(1 - x_{\text{Ge}})^2}, \quad (2)$$

where n_S and n_G are the Bose factors for the Si-Si and Ge-Ge phonons. At the same time, the frequency of the Si-Si mode in SiGe alloys is strongly dependent on Ge content x_{Ge} and is linear in x_{Ge} . The reported values of $b_{\text{Si-Si}}$ are mostly in the range of -700 to -1050 cm^{-1} .¹³ From the intensity ratio of the Ge-Ge mode to the Si-Si mode, the average Ge contents in annealed dots at 650, 700, and 800 °C can be obtained to be 0.57, 0.40, and 0.28, respectively, and average strains in annealed dots are obtained as -2.3% , -1.6% , and -1.2% from the peak position of the Si-Si mode, when $b_{\text{Si-Si}} = -980 \text{ cm}^{-1}$ is used for SiGe alloys with a low Ge composition ($x_{\text{Ge}} < 0.6$).²⁶ The values of the strain and composition in Si/Ge dots annealed at 650, 700, and 800 °C follow the relation $\varepsilon_{xx} = -0.042 x_{\text{Ge}}$ for pseudomorphic, biaxial strained layers. This indicates that strain relaxation in core regions of small-sized annealed Si/Ge dots is weak.

In addition to the Ge-Ge mode at 307.5 cm^{-1} , Raman spectra of Si/Ge dots show a strong Ge-Si peak at 421.5 cm^{-1} . The Ge-Si and Ge-Ge modes exhibit very different behaviors of the frequency shift with annealing temperature, as shown in the inset to Fig. 3. The peak at 421.5 cm^{-1} may be the alloylike mode in Ge-rich regions or a localized interface mode at Si/Ge interface regions of Si/Ge dots. The frequencies of Ge-Si mode in strained SiGe alloys can be determined from that of the unstrained SiGe alloys and the corresponding strain-induced frequency shift. For unstrained SiGe alloys, the frequency of the Ge-Si mode shows a cusplike dependence on x_{Ge} .^{13,20} The frequency of Ge-Si alloy mode in unstrained $\text{Si}_{0.2}\text{Ge}_{0.8}$ alloys is about 402 cm^{-1} . For the as-grown Si/Ge dot sample, the strain-induced frequency shift of the Ge-Si alloy mode is calculated to about 19.5 cm^{-1} when the common phonon strain-shift coefficient $b_{\text{Ge-Si}}$ of -575 cm^{-1} is used for the Ge-Si mode.⁸ This is in excellent agreement with the observed value. We use also $b_{\text{Ge-Si}} = -575 \text{ cm}^{-1}$ to calculate the Ge-Si alloy modes in annealed dot samples after considering the cusplike behavior of the Ge-Si peak frequency on x_{Ge} . The calculated frequencies (arrows in Fig. 3) of the Ge-Si alloy mode in annealed dots at 650, 700, and 800 °C are 420, 416, and 411 cm^{-1} , respectively, which are very close to the observed values. Considering the fact that the annealing behavior of the Ge-Si mode in as-grown and annealed dots can be understood by the cusplike dependence of the Ge-Si frequency on x_{Ge} and the strain-induced frequency shift, the observed Ge-Si peak is related to the Ge-Si alloy mode in Ge-rich regions of Si/Ge dots and not to a Ge-Si localized interface mode in the interface regions around Si/Ge dots. The good agreement between the calculated and observed frequencies of Ge-Si alloy modes indicates that a phonon strain-shift coefficient of $b_{\text{Ge-Si}} = -575 \text{ cm}^{-1}$ is reasonable for the Ge-Si alloy mode in Si/Ge dots with high x_{Ge} . The small deviation between calculated and observed frequencies of the Ge-Si

mode for dot samples annealed at 700 and 800 °C may result from the variation of $b_{\text{Ge-Si}}$ for SiGe alloys with a low Ge content.

IV. DISCUSSIONS

The strain and composition obtained from the LO-TO frequency splitting of the Ge-Ge mode are in good agreement with those from the frequencies of 2TA and Si-Si modes in Si/Ge dots. Based on Vegard's law, the strain of $\sim -3.4\%$ in Ge-rich regions of Si/Ge dots corresponds to that of pseudomorphic $\text{Si}_{0.19}\text{Ge}_{0.81}$ alloys grown on (001) Si substrate. The almost same Ge composition in such SiGe alloys and Ge-rich regions of Si/Ge dots indicates that the elastic or inelastic strain relaxation in Ge-rich regions of as-grown Si/Ge dot layers is negligible in Raman spectra but Si/Ge intermixing is important. Moreover, we applied x-ray diffraction to the as-grown Si/Ge dot sample (not shown here). The average vertical strain in one periodic structure is about 0.26% relative to the bulk Si lattice parameter. A 10 ML $\text{Si}_{0.2}\text{Ge}_{0.8}$ alloy layer and 25-nm-nominal Si spacer layers give a good fit to the x-ray diffraction (XRD) data, and we get a strain in the alloy layers of $\bar{\epsilon}_{zz} = 5.2\%$. This vertical strain corresponds to an average lateral strain of -3.0% in alloy layers under a biaxial strain model, which is close to the strain gotten from the LO-TO frequency splitting of the Ge-Ge mode. For the as-grown and annealed small-sized Si/Ge dots, the strain relaxation is found to be small. All the results indicate that the average strain in as-grown and annealed small-sized Si/Ge dots can be well described by a biaxial strain induced by the different lattice parameters between substrate and epitaxial layer. Using the obtained strain and composition, we can estimate the phonon strain-shift coefficient $b_{\text{Ge-Ge}}$ for the Ge-Ge mode in the biaxial case. For $x_{\text{Ge}} = 0.80$ and 0.57 , we get $b_{\text{Ge-Ge}} = -400 \text{ cm}^{-1}$ and for $x_{\text{Ge}} = 0.28$, $b_{\text{Ge-Ge}} = -580 \text{ cm}^{-1}$, where the frequency of the Ge-Ge mode in unstrained SiGe alloys is taken from Ref. 20. The $b_{\text{Ge-Ge}}$ value of -400 cm^{-1} for $x_{\text{Ge}} > 0.55$ is very close to the value reported for bulk Ge by Cerdeira *et al.*²⁷

Besides the intensity ratio of the Ge-Ge and Si-Si modes, that of the Ge-Ge and Ge-Si ($I_{\text{Ge-Si}}$) modes is also used to determine the Ge content in Ge/Si alloys and nanostructures by the following equation,^{23,25,28}

$$\frac{I_{\text{Ge-Ge}}}{I_{\text{Ge-Si}}} = A \frac{x_{\text{Ge}}}{2(1-x_{\text{Ge}})}, \quad (3)$$

where different values (from 1 to 3.2) of A were used to calculate the Ge content. The frequency shift of Ge-Ge and Si-Si modes and the intensity change of the Si-Si mode with the annealing temperature indicate that the Ge content has significantly changed in Si/Ge dots due to the Ge/Si intermixing during the annealing process. The intensity ratio of the Ge-Ge and Ge-Si modes, however, is almost the same for Si/Ge dot samples annealed at 650, 700, and 800 °C. In fact, because of the different resonant behavior of the various modes in SiGe alloys, the parameter A may change with alloy composition and the wavelength of the exciting light. For a fixed wavelength of 457 nm, Eq. (3) cannot give a

good fit to the Ge content even when Ge composition is in a small range of 0.20–0.40.²⁸ Moreover, the small slope of the curve Eq. (3) will lead to a large error in determining the Ge composition. Therefore, it is not surprising that the intensity ratio of the Ge-Ge and Ge-Si modes cannot give a reliable Ge content value for the annealed Si/Ge dots. However, the relative intensity of the Ge-Ge mode to the Si-Si mode is proportional to $[x/(1-x)]^2$. This indicates that the sensitivity to errors in determining the composition from the relative intensity of these modes is much smaller compared to that of the Ge-Ge mode to the Ge-Si mode.

When the phonon strain-shift coefficients of the Ge-Ge, Ge-Si, and Si-Si modes are obtained, the frequencies of those modes can be used to probe the strain and composition in Ge(Si) alloys and nanostructures. The frequency shift $\Delta\omega_i$ of a Raman mode (i) in strained and unstrained Si/Ge systems is determined by the vertical strain ϵ_{zz} and the lateral strain ϵ_{xx} .²² Based on a biaxial strain model, the strain-induced frequency shift $\Delta\omega_i$ has a simple relation $\Delta\omega_i = b_i \epsilon_{xx}$ to the lateral strain ϵ_{xx} . Numerical calculations show that the strain relaxation in a single flat Si/Ge dot is different in lateral and vertical directions,^{4–6} and the stacking of correlated Si/Ge dots will significantly enhance strain relaxation.^{1,5} The different mechanisms of the strain relaxation in correlated Si/Ge dots and large-size Si/Ge dots may result in strain in Si/Ge dots diverging from a biaxial strain model. In this case, the ratio and contribution of vertical and lateral strain components in Si/Ge dots directly affect the phonon strain-shift coefficient of a Raman mode in Si/Ge dots. Thus, different sets of phonon strain-shift coefficients of Raman modes are needed to determine the average strain and composition in correlated Si/Ge dot multilayers and large-sized Si/Ge dots.

The values of Ge content and strain ϵ_{xx} deduced from Raman spectra are very valuable for understanding important properties of Si/Ge dot structures, such as the effective band gap and band offsets. A photoluminescence transition energy of 0.74 eV observed in the studied sample at low temperature, for example, can be understood only by taking into account a quantum confinement energy of hole states within the small-sized quantum dots of about 170 meV. The complex local strain fields surrounding the dots that are caused by elastic strain relaxation appear to affect the average dot properties not significantly. The detailed quantum level scheme, however, will be influenced by the local profiles of Ge content and strain of individual Si/Ge dot. For Raman studies of dot layer samples, such local profiles, Si/Ge interface regions as well as segregated Ge within Si spacer layers may contribute just to phonon line broadening that cannot be resolved.

Here, we have shown that three methods can be used to get the strain and composition in uncorrelated small-sized Si/Ge dots. The first one is detecting the frequency of 2TA mode and the frequency of the Si-Si alloy mode in Si/Ge dots if they can be observed in Raman spectra. The second one is measuring the intensity ratio of the Ge-Ge and Si-Si modes and the frequency of the Si-Si alloy mode. The last one is determining the frequency and the LO-TO frequency splitting of the Ge-Ge mode. If one can observe the 2TA and Si-Si alloy modes in Si/Ge dots, it is very useful to use the

two modes to get the strain and composition. For a Si/Ge dot multilayer structure, the LO-TO frequency splitting of the Ge-Ge mode can further provide the information of the strain components along the lateral and vertical directions if the Ge composition in Si/Ge dots is beforehand determined. If the relaxation of the average strain in Si/Ge dots does not follow the biaxial model, the Ge content obtained from the frequency and the LO-TO frequency splitting of the Ge-Ge mode under a biaxial model will be larger than the original value. For example, for about 8% lateral and 20% vertical relaxation representing a typical local maximum in Si/Ge dots,^{1,5} we calculate $x_{\text{Ge}}=0.87$ compared to the original value of 0.82 if the biaxial case is assumed in the calculation. If the Si/Ge dot multilayers are not thick enough to observe the LO-TO frequency splitting of optical modes by micro-Raman measurements at a polished facet, the results show that within the biaxial model, the Ge content and strain in Si/Ge dots with a high Ge content can be obtained from the frequency of Ge-Ge and Ge-Si modes after considering the phonon strain-shift coefficients of $b_{\text{Ge-Ge}} = -400 \text{ cm}^{-1}$ and $b_{\text{Ge-Si}} = -575 \text{ cm}^{-1}$ and the cusplike behavior of Ge-Si alloy mode in unstrained SiGe alloys.

V. CONCLUSIONS

Raman scattering of the optical phonon modes in as-grown and annealed spatially uncorrelated Si/Ge dot multilayers is reported in detail. A second-order transversal acoustic (TA) mode at $\sim 170 \text{ cm}^{-1}$ and a second-order optical Ge-Ge mode at $\sim 595 \text{ cm}^{-1}$ are observed. A frequency splitting of 4.2 cm^{-1} between the LO and TO Ge-Ge peaks in

Si/Ge dots is observed in Raman spectra. An average Ge content of about 0.8 and lateral strain of about -3.4% are consistently determined in as-grown Si/Ge dots with a height of about 2 nm from the LO-TO splitting of the Ge-Ge mode and other spectral features. It clearly indicates that a certain amount of intermixing takes place between Si spacer layers and Si/Ge dots in Si/Ge dot multilayer structures. The Raman results also indicate that the strain relaxation in Ge-rich regions of small-sized Ge dots is weak and that the variation of Si content and strain in the core regions of the as-grown and annealed Si/Ge dots is small. The annealing behavior of the Ge-Si mode indicates that the observed sharp Ge-Si mode is a Ge-Si alloy mode in the core regions of Si/Ge dots, rather than a Ge-Si interface mode in the interface regions of dots. It is found that the intensity ratio of the Ge-Ge and Ge-Si modes cannot give a reliable Ge content value for the annealed small-sized Si/Ge dots. The phonon strain-shift coefficients of the Ge-Si and Ge-Ge modes are obtained for such Si/Ge dots with a high Ge content. The results suggest that a biaxial strain model is enough to understand the optical phonon peak frequencies and the observed LO-TO splitting of the Ge-Ge mode in small-sized Si/Ge dots.

ACKNOWLEDGMENTS

The authors would like to thank I. Bormann, A. Sticht, and H. Riedl for their experimental help in XRD measurement, sample growth, and sample annealing. This work was financially supported by the DFG (Grant No. BR1960/1-3) and the BMBF (Grant No. 13N7870).

*Electronic address: pinghengtan@hotmail.com

[†]Electronic address: Karl.Brunner@physik.uni-wuerzburg.de

¹K. Brunner, Rep. Prog. Phys. **65**, 27 (2002).

²S.H. Kwok, P.Y. Yu, C.H. Tung, Y.H. Zhang, M.F. Li, C.S. Peng, and J.M. Zhou, Phys. Rev. B **59**, 4980 (1999).

³O.G. Schmidt and K. Eberl, Phys. Rev. B **61**, 13 721 (2000).

⁴J.H. Seok and J.Y. Kim, Appl. Phys. Lett. **78**, 3124 (2001).

⁵O.G. Schmidt, K. Eberl, and Y. Rau, Phys. Rev. B **62**, 16 715 (2000).

⁶S. Christiansen, M. Albrecht, H.P. Strunk, and H.J. Maier, Appl. Phys. Lett. **64**, 3617 (1994).

⁷A. Milekhin, N.P. Stepina, A.I. Yakimov, A.I. Nikiforov, S. Schulze, and D.R.T. Zahn, Eur. Phys. J. B **16**, 355 (2000).

⁸J.H. Zhu, C. Miesner, K. Brunner, and G. Abstreiter, Appl. Phys. Lett. **75**, 2395 (1999).

⁹V. Magidson, D.V. Regelman, R. Beserman, and K. Dettmer, Appl. Phys. Lett. **73**, 1044 (1998).

¹⁰J. Groenen, R. Carles, S. Christiansen, M. Albrecht, W. Dorsch, H.P. Strunk, H. Wawra, and G. Wagner, Appl. Phys. Lett. **71**, 3856 (1997).

¹¹A.V. Kolobov, J. Appl. Phys. **87**, 2926 (2000).

¹²Paul A. Temple and C.E. Hathaway, Phys. Rev. B **7**, 3685 (1973).

¹³K. Brunner, in *Properties of Silicon Germanium and SiGe:C*, edited by E. Kasper and K. Lyutovich, EMIS Datareviews Series Vol. 24 (IEE, INSPEC, 2000), p. 115.

¹⁴Jeffrey S. Lannin, Phys. Rev. B **16**, 1510 (1977).

¹⁵D. Bougeard, P. H. Tan, M. Sabathil, P. Vogl, G. Abstreiter, and K. Brunner, Physica E (to be published).

¹⁶R. Schorer, G. Abstreiter, S. de Gironcoli, E. Molinari, H. Kibbel, and H. Presting, Phys. Rev. B **49**, 5406 (1994).

¹⁷S. de Gironcoli, Phys. Rev. B **46**, 2412 (1992).

¹⁸M. De Seta, G. Capellini, F. Evangelisti, and C. Spinella, J. Appl. Phys. **92**, 614 (2002).

¹⁹U. Denker, M. Stoffel, O.G. Schmidt, and H. Sigg, Appl. Phys. Lett. **82**, 454 (2003).

²⁰M.I. Alonso and K. Winer, Phys. Rev. B **39**, 10 056 (1989).

²¹M. Stoehr, D. Aubel, S. Juillaguet, J.L. Bischoff, L. Kubler, D. Bolmont, F. Hamdani, B. Fraisse and R. Fourcade, Phys. Rev. B **53**, 6923 (1996).

²²Z.F. Sui, I.P. Herman and J. Bevk, Appl. Phys. Lett. **58**, 2351 (1991).

²³M.A. Renucci, J.B. Renucci, and M. Cardona, in *Proceedings of the Second International Conference on Light Scattering in Solids*, edited by M. Balkanski (Flammarion, Paris, 1971), p. 326.

²⁴R. Schorer, E. Friess, K. Eberl, and G. Abstreiter, Phys. Rev. B **44**, 1772 (1991).

²⁵J.C. Tsang, P.M. Mooney, F. Dacol, and J.O. Chu, J. Appl. Phys. **75**, 8098 (1994).

²⁶D.J. Lockwood and J.M. Baribeau, Phys. Rev. B **45**, 8565 (1992).

²⁷F. Cerdeira, C.J. Buchenauer, F.H. Pollak, and M. Cardona, Phys. Rev. B **5**, 580 (1972).

²⁸P.M. Mooney, F.H. Dacol, J.C. Tsang, and J.O. Chu, Appl. Phys. Lett. **62**, 2069 (1993).